This article has been accepted for publication in a future issue of this journal, but has not been fully edited. Content may change prior to final publication. Citation information: DOI 10.1109/TNSRE.2014.2371339, IEEE Transactions on Neural Systems and Rehabilitation Engineering

Design of a Robotic System to Measure Propulsion Work of Over-ground Wheelchair Maneuvers

Howard Liles, Morris Huang, Jayme Caspall, and Stephen Sprigle

***Abstract*— A wheelchair-propelling robot has been developed to measure the efficiency of manual wheelchairs. The use of a robot has certain advantages compared to the use of human operators with respect to repeatability of measurements and the ability to compare many more wheelchair configurations than possible with human operators. Its design and implementation required significant engineering and validation of hardware and control systems. The robot can propel a wheelchair according to pre-programmed accelerations and velocities and measures the forces required to achieve these maneuvers. Wheel velocities were within 0.1 m/s of programmed values and coefficients of variation (CV) < 2%. Torque measurements were also repeatable with CV <10%. By determining the propulsion torque required to propel the wheelchair through a series of canonical maneuvers, task-dependent input work for various wheelchairs and configurations can be compared. This metric would serve to quantify the combined inertial and frictional resistance of the mechanical system.**

***Index Terms* — Anatomical, Mechanical Design, Inertia, Resistive Loss, Model, Power, Propulsion, Mechanical Torque, Repeatability, Robotic, Wheelchair**

I. Introduction

Wheelchair users maneuver using bouts of activity that are characterized by changes in speed and direction [1]. These changes in momentum are achieved by applying force to the pushrims and thus torque to the drive wheels. From a mechanical design standpoint, the major factors influencing propulsion effort are inertia and frictional energy losses. On a chair with greater inertia and/or greater frictional loss, the user will be required to exert greater instantaneous force and total effort while completing a maneuver. Greater effort can lead to difficulty in achieving desired speeds, a higher probability of fatigue over long bouts of mobility, and difficulty negotiating inclines. Over time, the accumulation of this greater effort can also increase the potential for injury in the upper extremities [2, 3], an observation that has been documented for almost 20 years.

These issues have motivated a substantial body of research targeting the biomechanics of wheelchair propulsion [4-7]. However, this field has yet to directly measure the mechanical work needed to maneuver manual wheelchairs (MWCs) during over-ground maneuvers.

Characterizing the mechanical work or “propulsion work” of wheelchairs is important to several stakeholder groups: wheelchair users, clinicians, manufacturers and insurance carriers. Users and clinicians will be more informed about equipment options based upon quantitative scientific knowledge about energy losses and propulsion effort specific to individual wheelchair types. Manufacturers can incorporate invaluable information during the design process and improve manufacturing techniques. Finally, insurance carriers will obtain an effective performance-based metric by which wheelchairs can be classified, allowing them to improve upon the current arbitrary weight classification system used in the United States.

This paper will describe the design and evaluation of a robotic system that is capable of propelling wheelchairs through various maneuvers with the goal of directly measuring the propulsion work of manual wheelchairs.

II. Current State of Knowledge

Studies of manual wheelchairs have focused on friction and inertial influences and produced useful information on rolling resistance as a function of wheelchair type [8, 9], caster size [10] and tire design and material [11-13]. The measurement and influence of mass and mass distribution has also been well described [14]. These studies describe component-level performance, often independent of their application to wheelchairs; however, component-level information does not translate fully to clinically-useful knowledge because testing typically does not reflect maneuvers relevant to a wheelchair’s environment, nor does it reflect the complex interaction of inertia and frictional energy loss. Thus, a systems level

This work was completed as part of the Mobility RERC, which is funded by the National Institute on Disability and Rehabilitation Research of the U.S. Department of Education under grant number H133E080003. The opinions contained in this manuscript are those of the grantee and do not necessarily reflect those of the U.S. Department of Education.

The authors acknowledge Phuc Dao for his efforts on the formative design and development of this system and Dr. Aldo Ferri for his insight during the design process.

H. J. Liles was with the Mechanical Engineering Department, Georgia Institute of Technology, Atlanta, GA 30332 USA. He is now with Pratt and Whitney, Hartford, CT 06118 USA (e-mail: hliles3@gatech.edu).

M. Huang is with the Mechanical Engineering Department, Georgia Institute of Technology, Atlanta, GA 30332 USA. (e-mail: mhuang@gatech.edu).

J. J. Caspall was with the Mechanical Engineering Department, Georgia Institute of Technology, Atlanta, GA 30332 USA. He is now with Lumense, Atlanta, GA 30308 USA (e-mail: jcaspall@lumense.com).

S. H. Sprigle is with the Applied Physiology and Industrial Design Departments, Georgia Institute of Technology, Atlanta, GA 30332 USA. (e-mail: stephen.sprigle@coa.gatech.edu).

This article has been accepted for publication in a future issue of this journal, but has not been fully edited. Content may change prior to final publication. Citation information: DOI 10.1109/TNSRE.2014.2371339, IEEE Transactions on Neural Systems and Rehabilitation Engineering

approach is necessary to evaluate the mechanical performance of wheelchairs.

Biomechanical studies of wheelchair propulsion also have a long history and have been important to define the means by which human operators impart forces onto the pushrims. Studies have attempted to: distinguish propulsion effort between wheelchairs with different designs and configurations [15, 16]; distinguish propulsion effort between wheelchairs with different mass, mass distribution, and tire type during steady-state propulsion [16]. Other studies have shown the impact of changing wheelchair configurations on the kinematics of pushrim usage [17], muscle activity [6, 18], velocity and acceleration [19], and the forces applied on the pushrim [20-22]. In addition, surface type [20, 23], tire type [24], and tire inflation [13] have been identified as factors influencing rolling resistance, and therefore, increased effort in propulsion. The majority studied propulsion using treadmills or roller systems, whereas only a few of these studies [13, 19-21] used over ground motion, but were limited to straight maneuvers. However, studying human operators has two key limitations if trying to develop a test method capable of measuring the propulsion work of manual wheelchairs.

The first limitation is that methodologies using straight-forward steady-state propulsion do not include the impact of all inertial changes and frictional influences on propulsion work. Maneuvering a wheelchair includes changes in speed and direction, which requires propulsion torque to overcome inertia and the energy losses due to friction. Therefore, the study of propulsion work must include changes in wheelchair momentum without impacting the inertia of the wheelchair, itself. Wheelchairs propelled on rollers and treadmills are not endowed with momentum nor are able to assess curvilinear trajectories. Instrumented wheels (i.e., SmartWheel; Optipush) add appreciable mass to the wheelchair system, thus impacting both inertia and friction during maneuvers that include accelerations, decelerations and turning [25].

A second limitation concerns the use of human subjects. The use of wheelchair users to study the biomechanics of propulsion is both valid and important. However, when studying a mechanical system, a more controlled and repeatable means for imparting energy is needed. Human operators simply add too much variability for use in a test method focused on characterizing the wheelchair performance. This can be due to differences in propulsion strokes and fatigue. These factors can confound measurements of the mechanical system. In fact, a number of studies have been unable to report differences in certain wheelchair configurations and their results have been, in part, attributed to variance from human operators [15, 16]. Moreover, test methods must be repeatable across testing sites, and the use of human operators would make it virtually impossible for one testing facility to recruit people who propel in the exact manner as a group of people recruited in a different testing facility.

To overcome these limitations, a robot has been designed to maneuver manual wheelchairs. By means of closed-loop velocity control, the system can execute wheelchair maneuvers precisely and repeatably. The correspondingly measured propulsion torque can then be used to calculate the average power or total work onto the drive wheels, quantifying the wheelchair's performance as a mechanical system. Moreover, this approach has the ability to make numerous valid and reliable measurements which are needed to study of the wide breadth of wheelchair designs and configurations.

III. METHODS

A. Design Criteria

The Anatomical Model Propulsion System (AMPS) is a robotic system designed to propel a MWC through maneuvers that reflect wheelchair usage in everyday life while measuring the applied propulsion forces and wheelchair kinematics.

The AMPS is designed to autonomously navigate predefined maneuvers that, together, encompass all the important dynamic response characteristics of manual wheelchair propulsion. Derived results - obtained from the recorded velocity, force, and current data - are a set of torques and work energies corresponding to the various maneuvers, which collectively characterize the wheelchair. They serve as a metric for comparing wheelchairs across classes and different models within a wheelchair class. Thus the AMPS will specifically target wheelchair design as opposed to evaluating human wheelchair biomechanics.

The following design criteria for the AMPS were defined: (1) the system should impart loads onto the wheels, axles, frame and upholstery of wheelchairs in a manner consistent with human operators; (2) it must propel the wheelchair in rectilinear and curvilinear maneuvers pertinent to broad characterization of human MWC performance; (3) the measurement instrumentation should be compatible with most commercially available wheelchairs; (4) data collection must measure the system input work and resultant kinetic energy during over-ground maneuvers; (5) the equipment should have minimal influence on the overall system mass and inertia; (6) the system should offer an acceptable precision of measurement defined as a coefficient of variation <15% with a goal of <10%; (7) it must be designed with materials and processes that are readily available in order to allow system

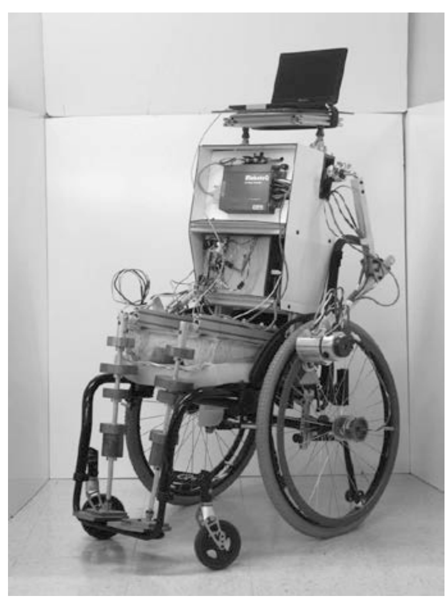

Fig. 1. The Anatomical Model Propulsion System (AMPS)

This article has been accepted for publication in a future issue of this journal, but has not been fully edited. Content may change prior to final publication. Citation information: DOI 10.1109/TNSRE.2014.2371339, IEEE Transactions on Neural Systems and Rehabilitation Engineering

replication.

The AMPS aims to meet these design criteria via three primary subsystems: the anthropomorphic structure, the propulsion system, and the data acquisition system.

B. System Design and Rationale

1) Anthropomorphic Design

The AMPS (Fig. 1) represents a human operator in an abstract form, and was designed to be consistent with the wheelchair dummy used in standardized test methods defined in ISO 7176-11 [26]. Using ISO 7176, the AMPS was designed with a mass of 100 kg to test typical adult size wheelchairs. Length parameters were defined by assessing the

TABLE I
AMPS Body Segment Parameters based on
100kg Wheelchair ISO Dummy and Hybrid III 50TH ATD

	Referenced metric	**Referenced value**	**Reference**
Segment Mass	Torso (including head, arms, trunk)	61±3 kg	ISO 7176-11
	Upper Legs (including pelvis & thighs)	31±3 kg	ISO 7176-11
	Lower Legs	7±1 kg	ISO 7176-11
	Total	100+5/-2 kg	ISO 7176-11
Center of Mass*	Trunk (x-axis or fore-aft)	68±10 mm	ISO 7176-11
	Trunk (z-axis or vertical)	298±10 mm	ISO 7176-11
	Upper Legs (x-axis)	203±10 mm	ISO 7176-11
	Upper Legs (z-axis)	67±10 mm	ISO 7176-11
	Lower Legs (vertical from foot)	235±3 mm	ISO 7176-11
Segment lengths	Seated Shoulder Height (from seat surface)	561 mm	Hybrid III 50th Male ATD
	Shoulder Breadth	455 mm	CAESAR Database
	Buttock to Knee Pivot	550 mm	Hybrid III 50th Male ATD
	Knee Pivot Height (from ground surface)	498 mm	Hybrid III 50th Male ATD
	Hip Breadth	414 mm	CAESAR Database

* Origin located at the midpoint of line formed by wheelchair seat and back planes intersecting.

ISO 7176 dummy and relating its dimensions to the anthropometry of the Hybrid III ATD [27] (Table I). Overall, the AMPS reflects the body segment parameters of an American male at the 50th percentile in height and 95th percentile in mass.

The size and weight specifications are utilized to capture the inertia of an occupied wheelchair and the interaction between the occupant and the wheelchair. This interaction primarily consists of loadings on the frame joints, the drive wheels and bearings, and the caster wheels and bearings. Matching the inertia and mass of the wheelchair user is vital, given that the user heavily influences the inertia and resistive losses within the wheelchair system.

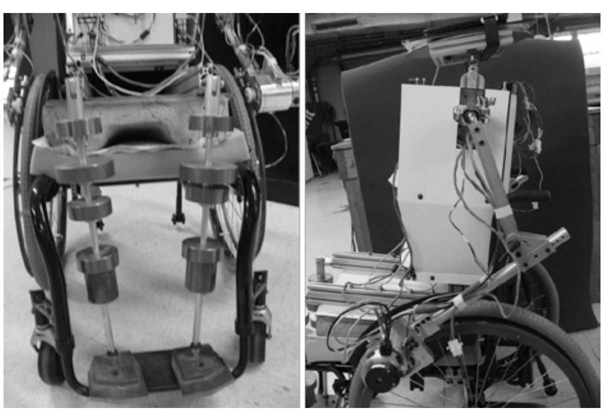

(a) (b)

Fig. 2. Anthropomorphic leg and arm structure. (a) AMPS leg structure incorporates weights to mimic mass distribution of human legs. (b) AMPS arm structure is designed to transmit loading from wheelchair rim to "shoulder" of the torso similar to a human user.

The AMPS torso structure is composed of an aluminum frame that houses the batteries which power the AMPS, and approximates upper body mass. A concrete mold shaped to match the mass and profile of the human posterior supports the torso structure. This mold connects to two aluminum rods which serve as the lower legs, as shown in Fig. 2. Weights are affixed along the length of these rods to mimic the mass distribution of the lower legs and feet. The arms are attached to the upper torso via a ball joint and are composed of aluminum tubing. The ball joints provide a significant range of adjustability for the positioning of the arms on various manual wheelchairs. At the end of these adjustable arms, the motor housings are attached. Of note is the fact that this modular design offers the flexibility to alter the mass and mass distribution of the AMPS in order to model different types of wheelchair users.

2) Propulsion Control

The AMPS propulsion system was designed to meet specifications by using tangential force drive, dedicated pushrim interfacing, and high-torque DC motors.

Manual wheelchairs are conventionally propelled by human users applying force to the pushrims. This applied force can be deconstructed to three force components: tangential, radial, and normal to the pushrim plane. In this case, only the tangential force performs work that contributes to propelling the wheelchair. However, humans are biomechanically constrained so that applying purely tangential force is impossible [28]. By applying purely tangential force to each pushrim, AMPS is able to isolate the efficiency of the mechanical design without the confounding inefficiencies associated with biomechanics. Additionally, the need to maneuver the wheelchair using differential and bidirectional drive led to the decision to use DC motors. Independent control of two DC motors enables turning and bidirectional motion, and the proximal motor mounting to the drive wheel offers a simple transmission. These motors contact the ring gears about 40 degrees forward of the top dead center of the drive wheel (Fig. 1). This "hand" position falls roughly in the center of a wheelchair user's contact with the pushrim during a propulsion stroke, making it coincident with where peak forces are applied in human kinetic studies [29].

To accommodate the variety of manual wheelchair pushrim styles, two design alternatives were considered: 1) design a propulsion system that would be compatible with all pushrim sizes and cross-section shapes [30], or 2) design a dedicated pushrim that can be attached to all wheelchairs during testing. The latter approach was selected because it offered a standard interface that enabled consistent force input, a more robust gripping mechanism, and an overall simpler design. This dedicated handrim is a PVC ring gear interfaced with the motors via a pinion gear, as depicted in Fig. 3. The ring gear has a mass of 0.75 pounds which is within the range of commercial pushrims, whose weights vary between 0.7 and 1.5 pounds.

This article has been accepted for publication in a future issue of this journal, but has not been fully edited. Content may change prior to final publication. Citation information: DOI 10.1109/TNSRE.2014.2371339, IEEE Transactions on Neural Systems and Rehabilitation Engineering

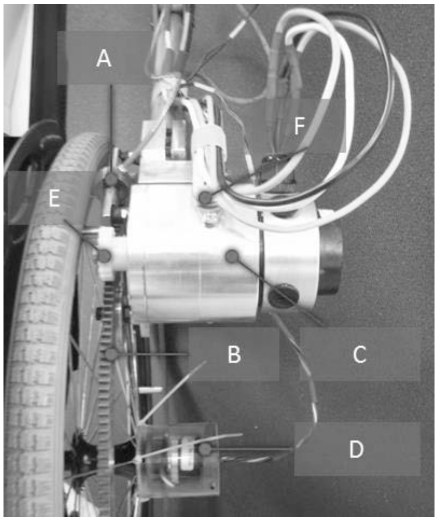

Fig. 3. Gear and sprocket interface between motor and pushrim. (A) force sensing load cell; (B) ring gear pushrim; (C) motor; (D) encoder mounted to drive wheel axle; (E) pinion gear; (F) bracket pivot.

DC motor specifications were based upon the torque demands required of over-ground motion. Literature sources indicate that the maximum tangential pushrim force applied during typical steady-state propulsion (~0.75 m/s) is less than 100N (22.5 lbf), and averages at 81N (18.2 lbf) [29]. Selection of an appropriate high-torque DC motor was based on matching the motor's peak efficiency torque to the nominal 81N, while assuming a pinion gear pitch diameter of 1.25-in. An additional constraint required that the motor max RPM achieve a minimal 0.75 m/s tangential velocity on the pinion gear during peak motor efficiency.

Based on these specifications, a pair of A28-150 Ampflow motors was chosen to provide propulsion to the wheelchair, with one for each drive wheel. The motors selected for this design meet the torque and speed requirements of the system and are contained with a specialized housing fixture that enable them to appropriately interface with the load cell sensor bracket. This bracket contains two components – a force-sensing load cell and a pivot axis for the motor – which work in conjunction to enable direct measurement of the tangential force applied to the pushrim. The motors are also directly attached to the AMPS arms so that the loading induced by action and reaction forces at the motor-pushrim interface will be translated to the upper torso via the shoulder joint in the same manner as would occur if the chair were being propelled by a human user. This enables the selected design to achieve realistic and representative loading on the MWC frame and upholstery. This configuration also enables widespread adaptability for a multitude of manual wheelchair designs and sizes.

The propulsion of the AMPS is controlled by a Roboteq motor controller. This controller is supplied power by a set of four 12-volt batteries and also serves as the interface through which the motors are powered. These internal batteries enable the AMPS to maneuver through a variety of environments without the need to connect to a local power source. This motor controller incorporates PID parameters and executes the closed loop control of the motor system. While all desired trajectories are programmed via a NI data acquisition (DAQ) device, all control of the motor is managed by the Roboteq controller. Upon receiving the input command from the NI device, the controller performs the necessary real-time calculations to incorporate the feedback from the motor encoders, and continuously sends the appropriate commands to the motor.

3) Data Acquisition

The requisite condition for calculating task propulsion work involves knowing the propulsion torque while monitoring system kinematics. Within the AMPS, this entails measuring the motor current, tangential pushrim force, and the rotational position of the drive wheels.

Measurement of the motor current is motivated by its proportionality with the motor torque. Two ACS758xCB current sensors are integrated into the circuit powering the drive motors by directly connecting to the motor power cables. Within this circuit, the sensors monitor the current flowing into the motors. The output reading is in the form of a voltage that is proportional to the current flowing through the sensors and is recorded by the DAQ. This data provides direct measurement of the energy that is input into the AMPS to execute the desired maneuvers.

Load cell measurement of the tangential pushrim force serves as a redundant system for determining the drive wheel torque. A pair of Omega LCFA-50 load cells are mounted onto a bracket connected to the motor housing unit. During propulsion, the reaction force of the gear teeth is tangential to the ring gear pushrim, requiring that the AMPS arm be positioned such that the load cell axis is parallel to the ring gear tangent. In this orientation, the propulsion force can be accurately measured by the load cell.

The AMPS incorporates a pair of M-260 Accu-Coder axle mounted encoders, each attached to the central axle of a drive wheel (as shown in Fig. 3) via a custom housing connector. These 2540 count encoders provide angular position data to the AMPS system, enabling precise measurement of the drive wheel motion. Using the known motion of the drive wheels with the predetermined geometry of the wheelchair, the full kinematics of the system can be derived for kinetic energy calculations [31].

A NI USB-6341 data acquisition system is used to record data and serves as the primary system controller for the AMPS. This DAQ connects to a computer via USB, and a Labview visual interface is used to communicate with the DAQ. The DAQ collects all the data from the AMPS drive wheel encoders, current sensors, and load cells. It also sends analog voltage signal commands to the Roboteq motor controller. The DAQ system is powered by a lithium-ion battery that is completely independent of the batteries supplying power to the AMPS propulsion subsystem.

C. Analytical Model of Wheelchair Efficiency

The propulsion work of manual wheelchairs goes towards storing mechanical energy and overcoming resistive energy losses. While the AMPS is capable of characterizing the task propulsion work, it is unable to directly partition the relative amounts of energy that go into overcoming inertia (or gravity) and resistive losses. However, by combining the encoder measurements and empirically measured wheelchair constants (e.g. mass, moment of inertia, wheelchair dimensions) in a

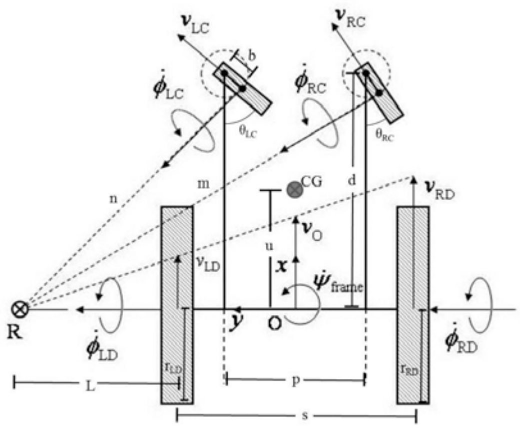

Fig. 4. Schematic for use in deriving wheelchair kinematics over ground

dynamic model, we can calculate the kinetic energy of the system, or the amount of energy stored as inertia. Assuming motion over flat ground (no potential energy), subtracting this value from the propulsion work quantifies the amount of resistive energy loss associated with the wheelchair system during a particular maneuver.

With respect to the dynamic model, the system kinetic energy (KE) is closely approximated by the summation of terms that contribute to the KE of linear travel, yaw (turning), and rotation of the drive wheels and casters. A complete description of this approach of determining the kinetic energy of a manual wheelchair and its validation has been reported in previous work [31] and will be briefly described here.

In essence, the wheelchair can be viewed as an assembly of 7 rigid bodies: frame, left and right drive wheels, left and right caster forks, and left and right caster wheels, as shown in Fig. 4. Maneuvering the wheelchair over ground requires force input to both drive wheels. Characterizing the motion of the drive wheels during over-ground maneuvers (measured by the rotary encoders) enables the determination of all other kinematic variables, except for caster orientation in some special cases. In addition to the kinematic variables, masses and moments of inertia must also be known. Yaw inertia of the system, $I_{ZZ,sys}^{G}$, and the system mass are measured experimentally using the inertia measurement device called the iMachine [32] that was developed for this purpose. This device is comprised of a spring loaded turntable on which large systems can be measured. When the device is given an initial displacement, the turntable will oscillate about the yaw axis of the system with the behavior of a damped simple harmonic system, from which the natural frequency and ultimately the yaw moment of inertia can be determined. For smaller components such as the wheelchair drive wheels and casters, a trifilar pendulum was constructed and used to measure the moment of inertia of these individual components about their rotational axes. The trifilar pendulum operates off of the same basic principle as the iMachine and has been widely documented in literature [33-35]. The trifilar pendulum provides greater sensitivity and resolution when measuring smaller objects due to the smaller device mass.

The kinetic energy, KE, of the wheelchair during over-ground motion on flat ground is the summation of the kinetic energy of its parts and can be determined via (1). Nomenclature is described by Fig. 4.

$$\begin{aligned} KE &= \tfrac{1}{2}m_{sys}{v_g}^2 + \tfrac{1}{2}I_{ZZ,sys}^{G}\dot{\Psi}_{frame}^2 + \tfrac{1}{2}I_{YY,LD}\dot{\phi}_{LD}^2 \\ &+ \tfrac{1}{2}I_{YY,RD}\dot{\phi}_{RD}^2 + \tfrac{1}{2}I_{YY,LC}\dot{\phi}_{LC}^2 + \tfrac{1}{2}I_{YY,RC}\dot{\phi}_{RC}^2 \\ &+ \tfrac{1}{2}I_{ZZ,LFLC}\,\dot{\Psi}_{LC}^2 + \tfrac{1}{2}I_{ZZ,RFRC}\,\dot{\Psi}_{RC}^2 \end{aligned} \tag{1}$$

The propulsion power required to perform a maneuver is calculated from the torque applied to the drive wheels via (2).

$$P_{in} = \tau\omega \tag{2}$$

In this case, P_{in} is input power in watts, τ is drive wheel torque in Newton-meters, and ω is drive wheel angular velocity in radians per second. The corresponding propulsion work can then be determined by integrating the propulsion power over the time interval of interest, as shown in (3).

$$W_{in} = \int_{t_i}^{t_f} P_{in}dt \tag{3}$$

The W_{in} represents the input work energy in joules, t_i is the maneuver start time in seconds, and t_f is the maneuver end time in seconds. By implementing the relationship expressed by (4), resistive energy loss, or E_{loss} can be quantified.

$$W_{in} = KE + E_{loss} \tag{4}$$

IV. Results

A. Calibration and Validation

Because the AMPS is a fundamentally new approach to measuring mechanical efficiency of wheelchairs, validating the hardware and measurement techniques was required. Specifically, the current sensor and load cells were individually calibrated, followed by system-level validation to investigate the repeatability of the commanded trajectory and measured propulsion torque during over-ground wheelchair maneuvers.

1) Component-level calibration

This article has been accepted for publication in a future issue of this journal, but has not been fully edited. Content may change prior to final publication. Citation information: DOI 10.1109/TNSRE.2014.2371339, IEEE Transactions on Neural Systems and Rehabilitation Engineering

Load cells. The force sensing load cells were calibrated in-situ with the instrumented wrist unit mounted to a specialized wheel designed to measure propulsion forces using a JR3 force transducer integrated into the pushrim with a solid ring gear attachment [36]. This instrumented wheel had been calibrated using precision weights. Load cell measurements were calibrated against instrumented wheel readings with the AMPS undergoing ramp-up ramp-down maneuvers on a dynamometer. Fig. 5 illustrates the measurements of the instrumented wheel's transducer and the AMPS load cell.

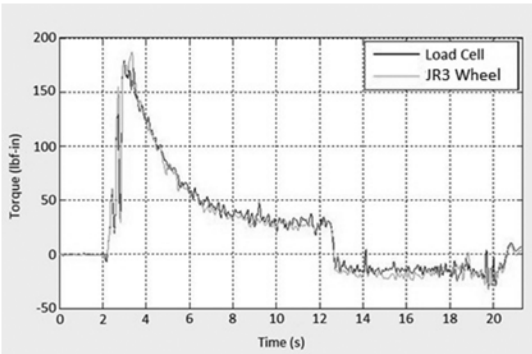

(a)

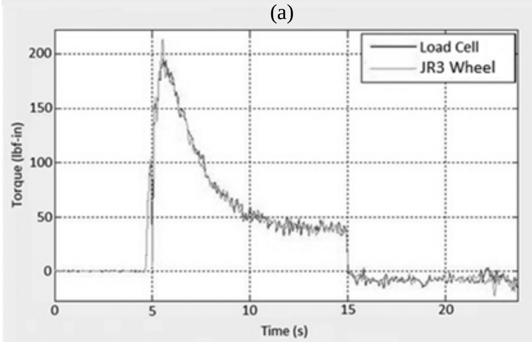

(b)

Fig. 5. Validating load cell data against calibrated torque-measurement wheel. (a) Recorded left motor torque. (b) Recorded right motor torque.

Current sensors. The current sensors were calibrated independently to determine calibration curves that correlate the measured torque to the actual torque supplied by the motors. This calibration was accomplished by loading the motors with a known torque by attaching a 3-inch diameter pulley to the motor shaft and using the motor as a winch to lift free-hanging weights of known mass. Several weights of varying mass were used to develop a calibration curve over a range of torques. The measured torques were calculated by scaling the recorded values using a linear constant provided on the manufacturer's specification sheet. The applied torques were determined by using mass of the weight, acceleration due to gravity and radius of the pulley. These two sets of torques were then plotted and a linear regression was fit to the data with R^2>0.99. Fig. 6 shows the calibration curves for the two motors. The resulting torque measurements correlate very closely with force measurements reported via the load cells during actual trial tests of the AMPS after the calibration had been completed. It is important to note that in Fig. 6, these torque values seem quite small because they represent the torque coming directly from the motor. The torque of interest, or the drive wheel torque, is determined by the following:

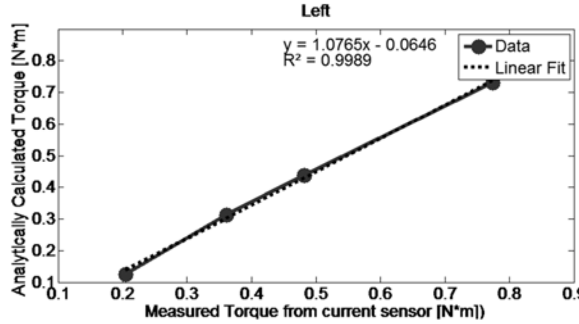

(a)

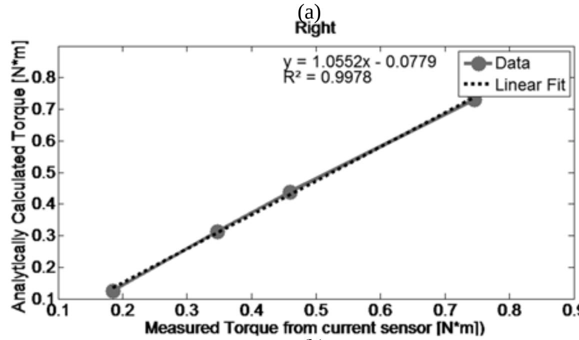

(b)

Fig. 6. Calibration curves for current sensor displaying calibration equations and R^2 values. (a) Left motor calibration curve. (b) Right motor calibration curve.

$$(F_{tan})_{wheel} = (F_{tan})_{motor} \quad (5)$$

$$\frac{\tau_{wheel}}{R_{ring\ gear}} = \frac{\tau_{motor}}{R_{pinion\ gear}} \quad (6)$$

$$\tau_{wheel} = \frac{R_{ring\ gear}}{R_{pinion\ gear}} \tau_{motor} \quad (7)$$

Note that $(F_{tan})_{wheel}$ and $(F_{tan})_{motor}$ are the tangential force on the ring gear and pinion gear, τ_{wheel} and τ_{motor} are the torques on the drive wheel and motor shaft, and $R_{ring\ gear}$ and $R_{pinion\ gear}$ are the pitch radii of the ring gear and pinion gear. Since the gear ratio between the ring gear and pinion gear is 17, the range of drive wheel torques the calibration procedure spans is about 2-Nm to 13-Nm, encompassing the bulk of torque values encountered during AMPS's over-ground maneuvers.

2) System-level calibration

Over-ground testing. The AMPS was also validated by performing maneuvers on a tile floor. The AMPS was loaded onto a Quickie GT manual wheelchair with 24" diameter, spoked, pneumatic tires. A straight maneuver was programmed, consisting of acceleration to a steady state speed over 2.5 seconds, maintaining this speed for 5 seconds, and then ramping down to a stop over 2.5 seconds. This maneuver was conducted at two speeds, 1.4 m/s and 0.7 m/s, and for a total of ten trials in each condition. These speeds represent greater than average velocities based upon measurements of wheelchair users during everyday mobility [1]. The maneuver was conducted ten times at each speed while measuring wheel velocity, current, and force data.

TABLE II
Repeatability of Velocity Trajectory

"Fast" 4.66 rad/s (1.4 m/s) maneuver				"Slow" 2.33 rad/s (0.7 m/s) maneuver		
	Left	Right			Left	Right
Coefficient of Variation [%]	1.05	1.06		Coefficient of Variation [%]	1.41	1.38
Standard Deviation [rad/s]	0.02	0.02		Standard Deviation [rad/s]	0.02	0.01
SEM [rad/s]	0.01	0.01		SEM [rad/s]	0.005	0.005

Control system accuracy was characterized by comparing the programmed velocity profile to the measured velocity profile and computing the error between the two waveforms (Fig. 7) every 0.5 seconds. Furthermore, the repeatability of the profile was characterized by determining the coefficient of variation of the entire maneuver for both the left and right wheels at both speeds (Table II). Velocity error was ≤0.1 m/s for both the left and right wheels across both speeds.

Propulsion torque metrics included peak acceleration, peak deceleration and the average steady state torque. Repeatability of propulsion torque (Table III) was assessed for repeatability using the coefficient of variation (CV) and standard error of the mean (SEM). As indicated by the values in Table II, the AMPS control scheme can deliver an accurate velocity profile

TABLE III
Torque Repeatability (Derived from Motor Current)

		Left Drive Wheel Torque (Nm)		
speed		peak accel	|peak decel|	steady-state average
1.4 m/s	mean	15.25	11.37	2.65
	standard deviation	0.66	0.60	0.07
	CV (%)	4.10	5.02	2.39
	SEM	0.21	0.19	0.02
0.7 m/s	mean	9.29	4.95	2.23
	standard deviation	0.44	0.49	0.14
	CV (%)	4.46	9.40	6.11
	SEM	0.13	0.15	0.05
		Right Drive Wheel Torque (Nm)		
speed		peak accel	|peak decel|	steady-state average
1.4 m/s	mean	12.44	12.70	1.71
	standard deviation	0.56	0.55	0.04
	CV (%)	4.30	4.10	2.27
	SEM	0.18	0.17	0.01
0.7 m/s	mean	6.80	5.95	0.94
	standard deviation	0.49	0.38	0.07
	CV (%)	6.83	6.11	7.18
	SEM	0.15	0.12	0.02

and the system can reliably measure propulsion torque during over-ground maneuvers. The CVs of the current-based torque were <5% during acceleration, <10% during deceleration and <8% during steady state velocity. Force data corresponded closely to the current-based torque, but was significantly noisier.

V. DISCUSSION

The results of testing indicate that the AMPS can maneuver a wheelchair within a tight trajectory profile and measure propulsion torques reliably. Across a series of trials, the CV of the measured angular velocity profile was less than 2%. The CV of the current-based torque meets the system's precision of measurement goal, with maximum CV values being less 10%, and with average CV values less than 5% in several cases. The accuracy and repeatability of the velocity profile ensures that the AMPS can successfully complete desired maneuvers in a consistent fashion.

Propulsion torques and work energies are influenced by the wheelchair occupant and the maneuvers being performed. AMPS affords the ability to load the wheelchair and perform the same maneuver in a repeatable manner. However, the resulting energetic measurements are reflective of these parameters. Different masses, speeds, or accelerations would result in different amounts of propulsion work. This is true for all studies on propulsion, whether using AMPS or human operators. Because it was designed to focus on the mechanical system, AMPS offers the capability to change these parameters easily and reliably. Mass of AMPS can be scaled upward or downward, and the maneuver trajectories, speeds, and accelerations can be changed to represent different types of users moving about in different manners. The AMPS design and the tested maneuvers were based upon documented rationale, but the reported propulsion torques and work energies are specific to the mass and inertia of the AMPS and the maneuvers under study.

Iterative design of the AMPS and validation of the system have allowed us to meet the defined design criteria. (1) By following an anthropomorphic design, the system accurately reflects human static loads and inertias, and feature realistic pushrim propulsion that allows propagation of reaction forces along upper limbs to the torso. (2) Independent control of bilateral DC motors using a robotic controller enables straight and turning maneuvers characteristic of everyday MWC maneuvers. (3) Multiple degrees of freedom in the upper limb joints and incorporation of a dedicated pushrim interface ensure broad compatibility of the AMPS propulsion system across a wide range of wheelchairs. (4) Load cells and current sensors grant the capacity to determine input system torque

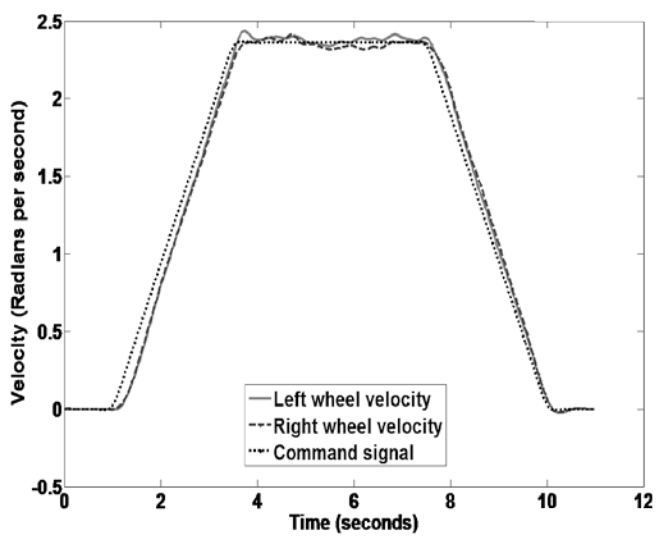

Fig. 7. Angular velocity profile of drive wheels at 2.33-rad/sec. For a set of 24" diameter drive wheels, equates to straight line motion of wheelchair at 0.7-m/s.

and work, while wheel encoders are used in conjunction with a kinematic model to derive system kinetic energy. (5) The propulsion and data acquisition system are incorporated as part of the anthropometric design, thus not shifting the system mass and inertia from its anthropomorphic bounds. (6) System validation has demonstrated a high-level of AMPS controllability and repeatability, yielding < 2% CV in straight maneuver velocities across ten trials, and <10% CV in imparted torques for the same maneuvers. (7) Assembly of the AMPS from commercially available material (80-20) and electronics (Roboteq, National Instruments) enables the replication of the system for widespread industrial testing, with a component cost of $6000 per unit. As a result, these design choices have culminated into the conception of a system that can reliably and repeatably evaluate MWC efficiency.

VI. Conclusion

The AMPS exhibited a high level of repeatability in controlling wheelchair velocity and in measuring the torque required to perform maneuvers, indicating the AMPS is a reliable test bed for quantitatively assessing how manual wheelchair systems respond to energy input from the user. The long term goal of this research is to accurately document the mechanical performance of manual wheelchairs to better inform wheelchair prescriptions. Given the breadth of wheelchair designs, frame materials, wheel and tire options, and axle positions, users (and their clinicians) need to be informed of how these options impact the effort required to propel wheelchairs. The selection of wheelchair type, components, and configurations involves negotiating a series of compromises, because these choices have tradeoffs in performance, function, cost, complexity, and a host of other factors. By understanding the impact that certain configurations have on propulsion work and efficiency, users become more empowered to make choices reflective of their idiosyncratic needs and desires.

VII. Future Work

Future considerations for the AMPS include addition of different control schemes and the ability to represent a wider variety of human users. More advanced control algorithms that incorporate trajectories with varying radii of curvature and directional changes will permit fuller assessment of the frictional and inertia influences on propulsion torque. Developing a control algorithm for producing a pulsatile propulsion torque will permit fuller assessment of the influence of propulsion techniques and strategies. Designing the capability to change mass and mass distribution will permit a means to represent different types of wheelchair users. Finally, an extensive series of tests comparing wheelchair configuration, wheel type, and wheelchair type will be conducted to achieve the long term goals of this research endeavor.

References

[1] Sonenblum SE, Sprigle S, and Lopez RA, "Manual Wheelchair Use: Bouts of Mobility in Everyday Life," *Rehabilitation Research and Practice*, pp. 7, 2012.

[2] M. L. Boninger, B. E. Dicianno, R. A. Cooper, J. D. Towers, A. M. Koontz, and A. L. Souza, "Shoulder magnetic resonance imaging abnormalities, wheelchair propulsion, and gender," *Arch Phys Med Rehabil*, vol. 84, no. 11, pp. 1615-20, Nov, 2003.

[3] van der Woude LHV, Dallmeijer AJ, Janssen TWJ, and Veeger D, "Alternative modes of manual wheelchair ambulation: An overview," *Am J Phys Med Rehabil* vol. 80, pp. 765-777, 2001.

[4] S. de Groot, H. E. Veeger, A. P. Hollander, and L. H. van der Woude, "Effect of wheelchair stroke pattern on mechanical efficiency," *Am J Phys Med Rehabil*, vol. 83, no. 8, pp. 640-9, Aug, 2004.

[5] M. L. Boninger, M. Baldwin, R. A. Cooper, A. Koontz, and L. Chan, "Manual wheelchair pushrim biomechanics and axle position," *Arch Phys Med Rehabil*, vol. 81, no. 5, pp. 608-13, May, 2000.

[6] Gutierrez DD, Mulroy S, Newsam CJ, Gronley JK, and Perry J, "Effect of fore-aft seat position on shoulder demands during wheelchair propulsion: part 2. An electromyographic analysis.," *J Spinal Cord Med*, vol. 28, no. 3, pp. 222-9, 2005.

[7] L. van der Woude, Hendrich, KM, Veeger, HEJ, van Ingen Schenau, GJ, Rozendal, RH, De Groot, G, Hollander, AP, "Manual wheelchair propulsion: effects of power output on physiology and technique," *Med Sci Sports Exerc*, vol. 20, no. 1, pp. 70-78, 1988, 1988.

[8] J. Thacker, and K. Foraiati, *Ride Comfort*, University of Virginia Rehabilitation Engineering Center Annual Report, 1991.

[9] L. H. van der Woude, C. Geurts, H. Winkelman, and H. E. Veeger, "Measurement of wheelchair rolling resistance with a handle bar push technique," *Journal of Medical Engineering & Technology*, vol. 27, no. 6, pp. 249-258, 2003.

[10] T. G. Frank, and E. W. Abel, "Measurement of the turning, rolling and obstacle resistance of wheelchair castor wheels," *J Biomed Eng*, vol. 11, no. 6, pp. 462-6, Nov, 1989.

[11] J. Gordon, J. J. Kauzlarich, and J. Thacker, "Tests of two new polyurethane foam wheelchair tires," *Journal of Rehabilitation Research and Development*, vol. 26, pp. 33-46, 1989.

[12] J. Kauzlarich, Thacker JG, "Wheelchair tire rolling resistance and fatigue," *Journal of Rehabilitation Research and Development*, vol. 22, no. 3, pp. 25-41, 1985.

[13] B. J. Sawatzky, I. Denison, and W. O. Kim, "Rolling, rolling, rolling," *Rehab Management*, vol. 9, pp. 36-39, 2002.

[14] C. Brubaker, "Ergonometric considerations," *J Rehabil Res Dev Clin Suppl*, no. 2, pp. 37-48, 1990.

[15] J. H. Bednarczyk, and D. J. Sanderson, "Limitations of kinematics in the assessment of wheelchair propulsion in adults and children with spinal cord injury," *Physical therapy*, vol. 75, no. 4, pp. 281-287, April 1995, 1995.

[16] C. E. Beekman, L. Miller-Porter, and M. Schoneberger, "Energy cost of propulsion in standard and ultralight wheelchairs in people with spinal cord injury," *Physical therapy*, vol. 79, no. 2, pp. 146-158, February 1999, 1999.

[17] Gorce P, and Louis N, "Wheelchair propulsion kinematics in beginners and expert users: Influence of wheelchair settings. ," *Clinical Biomechanics* vol. 27, pp. 7-15, 2012.

[18] N. Louis, and P. Gorce, "Surface electromyography activity of upper limb muscle during wheelchair propulsion: Influence of wheelchair configuration," *Clin Biomech (Bristol, Avon)*, vol. 25, no. 9, pp. 879-85, Nov, 2010.

[19] Freixes O, Fernández SA, Gatti MA, Crespo MJ, Olmos LE, and Rubel IF, "Wheelchair axle position effect on start-up propulsion performance of persons with tetraplegia," *Journal of Rehabilitation Research and Development* vol. 47, no. 7, pp. 661-668, 2010.

[20] Cowan RE, Nash MS, Collinger JL, Koontz AM, and Boninger ML, "Impact of surface type, wheelchair weight, and axle position on wheelchair propulsion by novice older adults. ," *Arch Phys Med Rehabil* vol. 90, pp. 1076-83, 2009.

[21] Kotajarvi BR, Sabick MB, An KN, Zhao KD, Kaufman KR, and Basford JR, "The effect of seat position on wheelchair propulsion

biomechanics," *J Rehabil Res Dev*, vol. 41, no. 3b, pp. 403-414, May/June, 2004.

[22] Mulroy SJ, Newsam CJ, Gutierrez DD, Requejo P, Gronley JK, Haubert LL, and Perry J, "Effect of fore-aft seat position on shoulder demands during wheelchair propulsion: part 1. A kinetic analysis. ," *J Spinal Cord Med*, vol. 28, no. 3, pp. 214-21, 2005.

[23] Koontz AM, Roche BM, Collinger JL, Cooper RA, and Boninger ML, " Manual wheelchair propulsion patterns on natural surfaces during start-up propulsion.," *Arch Phys Med Rehabil.*, vol. 90, no. 11, pp. 1916-23, 2009.

[24] Kwarciak AM, Yarossi M, Ramanujam A, Dyson-Hudson TA, and Sisto SA, "Evaluation of wheelchair tire rolling resistance using dynamometer-based coast-down tests.," *Journal of Rehabilitation Research and Development*, vol. 46, no. 7, pp. 931-938, 2009.

[25] S. Sprigle, "On "impact of surface type, wheelchair weight, and axle position on wheelchair propulsion by novice older adults"," *Arch Phys Med Rehabil*, vol. 90, no. 7, pp. 1073-5, Jul, 2009.

[26] International Standards Organization, "ISO 7176 Wheelchair Standards- Section 11: Test Dummies," International Standards Organization,, 2008.

[27] Foster J, Kortge J, and Wolanin M, *"Hybrid III-A Biomechanically-Based Crash Test Dummy*,, 1977.

[28] Rozendaal LA, Veeger HE, and van der Woude LH, "The push force pattern in manual wheelchair propulsion as a balance between cost and effect," *J Biomech.*, vol. 36, no. 2, pp. 239-47, 2003.

[29] R. N. Robertson, M. L. Boninger, R. A. Cooper, and S. D. Shimada, "Pushrim forces and joint kinetics during wheelchair propulsion," *Arch Phys Med Rehabil*, vol. 77, no. 9, pp. 856-64, Sep, 1996.

[30] M. L. van der Linden, L. Valent, H. E. G. Veeger, and L. H. V. van der Woude, "The effect of wheelchair handrim tube diameter on propulsion efficiency and force application (tube diameter and efficiency in wheelchairs)," *IEEE Transactions on Rehabilitation Engineering*, vol. 4, no. 3, pp. 123-132, September 1996, 1996.

[31] F. Medola, P. Dao, J. Caspall, and S. Sprigle, "Partitioning Kinetic Energy during Freewheeling Wheelchair Maneuvers," *IEEE Trans Neural Syst Rehabil Eng*, Nov 6, 2013.

[32] M. R. Eicholtz, J. J. Caspall, P. V. Dao, S. Sprigle, and A. Ferri, "Test method for empirically determining inertial properties of manual wheelchairs," *J Rehabil Res Dev*, vol. 49, no. 1, pp. 51-62, 2012.

[33] Du Bois JL, Lieven NA, and Adhikari S, "Error analysis in trifilar inertia measurements. ," *Exper Mech.*, vol. 49, no. 4, pp. 533-40, 2009.

[34] Hou ZC, Lu Y, Lao Y, and Liu D, "A new trifilar pendulum approach to identify all inertia parameters of a rigid body or assembly. ," *Mechanism Machine Theory.*, vol. 44, no. 6, pp. 1270-80, 2009.

[35] P. L. Ringegni, M. D. Actis, and A. J. Patanella, "An experimental technique for determining mass inertial properties of irregular shape bodies and mechanical assemblies," *Measurement*, vol. 29, no. 1, pp. 63-75, 1//, 2001.

[36] W. Limroongreungrat, Y. T. Wang, L. S. Chang, M. D. Geil, and J. T. Johnson, "An instrumented wheel system for measuring 3-D pushrim kinetics during racing wheelchair propulsion," *Res Sports Med*, vol. 17, no. 3, pp. 182-94, 2009.